A Smart Healthcare System Using Consumer Electronics and Federated Learning to Automatically Diagnose Diabetic Foot Ulcers

Sujit Kumar Das[1], Nageswara Rao Moparthi[2]*, Suyel Namasudra[3], Rubén González Crespo[4]*, David Taniar[5]

[1] Department of Computer Science and Engineering, Institute of Technical Education and Research, Siksha 'O' Anusandhan Deemed to be University, Bhubaneswar, 751030, Odisha (India)
[2] Amrita School of Computing, Amrita Vishwa Vidyapeetham, Andhra Pradesh, Amaravati Campus (India)
[3] Department of Computer Science and Engineering, National Institute of Technology, Agartala, Tripura (India)
[4] Universidad International de La Rioja, Logroño (Spain)
[5] Faculty of Information Technology, Monash University (Australia)

* Corresponding author: mnrphd@gmail.com (N. R. Moparthi), ruben.gonzalez@unir.net (R. González Crespo).

Abstract

Privacy breaches on sensitive and widely distributed health data in consumer electronics (CE) demand novel strategies to protect privacy with correctness and proper operation maintenance. This work presents a scalable Federated Learning (FL) framework-based smart healthcare approach. Remote medical facilities frequently struggle with imbalanced datasets, including intermittent client connections to the FL global server. The proposed approach handled intermittent clients with diabetic foot ulcers (DFU) images. A data augmentation approach proposes to handle class imbalance problems during local model training. Also, a novel Convolutional Neural Network (CNN) architecture, ResKNet (K=4), is designed for client-side model training. The ResKNet is a sequence of distinctive residual blocks with 2D convolution, batch normalization, LeakyReLU activation, and skip connections (convolutional and identity). The proposed approach is evaluated for various client counts (5,10,15, and 20) and multiple test dataset sizes. The proposed framework can leverage consumer electronic devices and ensure secure data sharing among multiple sources. The potential of integrating the proposed approach with smartphones and wearable devices to provide highly secure data transmission is very high. The approach also helps medical institutions collaborate and develop a robust patient diagnostic model.

Keywords

I. Introduction

TECHNOLOGICAL advancements and globalization result in massive data collection by various enterprises and organizations using consumer electronic devices. The use of CE devices in data collection provides a great help in facilitating better service to humans. These data include a Wide range of information, from financial and industrial to medical records. However, in the case of medical records, the data transmissions from patients require more careful strategies. [1]. The greater demand for in-depth analysis of these vast data influx results in various advancements in machine learning (ML) and deep learning (DL) strategies [2], [3]. However, given the value of this information, ensuring the confidentiality and security [4] of the analyzed data is of utmost importance [5]. Adherence to regulatory requirements, such as the General Data Protection Regulation (GDPR)

[6], becomes mandatory in many instances. The traditional method for applying ML to decentralized data comprises a centralized framework sharing data by various entities, shown in Fig. 1. The client must transfer data to a centralized server for model training and subsequent results. Thereby, each client gets the final results. One of the major disadvantages of this approach is data confidentiality and the attributes related to it [7]. Furthermore, it requires a high bandwidth and low latency communication infrastructure to handle predictions promptly and successfully. One potential solution is each data owner possesses the model, so transferring data is not required when new information becomes accessible [8], [9]. It can decrease latency by making predictions for each client individually. Also, it reduces network reliance, lowering communication expenses. Nevertheless, each client must transmit data to the central server for the initial training of the model [10]. Although multiple traditional ML approaches are introduced to design
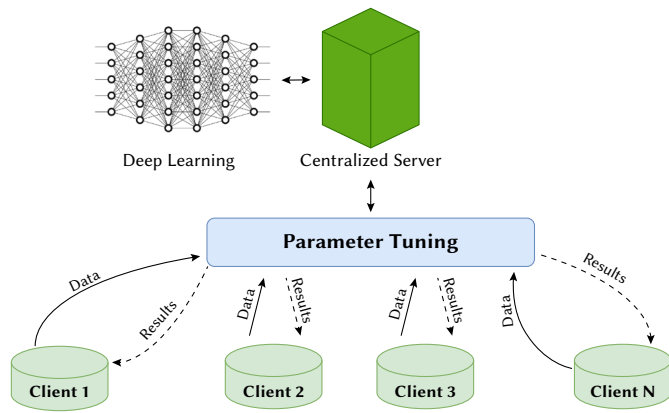
Fig. 1. Traditional centralized learning.

data-driven DFU identification systems, most systems are centralized frameworks and work on imbalanced class labels. An approach has yet to consider a decentralized technique for model training. FL [11] gains popularity as a practical approach to guarantee that data remains on the servers of specific data owners, even throughout the training process [12]. It preserves essential data privacy when acquiring data locally from clients for centralized training is impossible [13]. FL does data analysis in a decentralized approach to avoid sending user data to central servers [14]. The primary motivation of this work is to address the disparity between advanced ML methods and real-world applicable conservative, large-scale healthcare solutions, taking better care of patient privacy and improving diagnostic performance in low-resource settings. To build such a robust system that can be put into practice on consumer devices for healthcare, the learning process has to be offloaded, and data sharing has to be internalized using federated learning. The development of DFU often leads to complications such as neuropathy and arterial disease in the lower extremities [15]. It is imperative to harness advanced ML, DL, and computer vision techniques to assist clinicians in accurately diagnosing DFU, thereby enhancing patient care. The identification of DFU using ML and DL techniques is introduced in various works. In one such work [16], a two-stage ML classification approach is proposed that analyzed foot thermograms. In another work [17], a novel parallel convolution layer-based CNN architecture (DFUNet) is proposed for differentiating between normal and abnormal DFU wounds. DFU_QUTNet [18], a CNN architecture is introduced for extracting multi-level features, which are subsequently input into Support Vector Machine (SVM) and K-Nearest Neighbours (KNN) classifiers. The hybridization of Neural Networks (NN) and Bayesian Classifiers (BNC) to detect necrotic tissue in wounds [19]. A dedicated DL-based model [20] for wound image segmentation with wound detection is also considered as a significant approach. Traditional ML approaches like a 2-level SVM classifier [21] for determining wound boundaries. In a study, standard CNN architectures [22] were employed for DFU wound segmentation. Later, a new dataset with ground truth labels for ischaemia and infection recognition [23].

This paper uses FL to investigate medical images and make predictions. While predictions are made, different numbers of clients and test image samples are considered. The proposed approach is decentralized by a training model with local augmented data. The local clients learn from the data they acquire and share the knowledge with other clients. At first, the imbalance data are augmented using a hybridized oversampling approach with combined capabilities of both SMOTE (Synthetic Minority Oversampling TEchnique) and SVM-SMOTE (Support Vector Machine-synthetic Minority Oversampling TEchnique). The proposed augmentation approach helps generate suitable synthetic data from the minority class and improves client

learning. The local machine update (LMU) is then sent to FL for global machine update (GMU). This collaborative approach helps better learning and provides a more realistic approach to ischaemia and infection identification in DFU with data privacy. The key contributions of the proposed method are as follows:

1. The use of FL to diagnose DFU without sharing sensitive data or related information in a remote healthcare setting to improve privacy and security.

2. A hybridized data augmentation technique is proposed to expand and balance the class distribution of the samples and examine the impact of the proposed augmentation approach on the collaborative framework.

3. A deeper residual block-based shallow CNN architecture that requires less computational resources for client-side model training.

4. The presence of decentralized data and the uneven distribution resulting from intermittent clients, the proposed architecture exhibits robustness and yields superior performance.

The remaining work sections are: Section II includes related works, and section III includes detailed problem definition and system model. Section IV offers a detailed description of the proposed methodology, outlining the key elements of the approach. Section V carries out experiments and provides detailed explanations, shedding light on the experimental process and results. Finally, section VI serves as the paper's conclusion, summarising the essential findings and insights gathered throughout the work.

II. Related Works

The development of DFU often leads to complications such as neuropathy and arterial disease in the lower extremities. It has been estimated that approximately 50%of DFU patients will experience neuropathy-related issues in later stages, with around 20% of them developing arterial blood flow problems. As many as 80% may suffer from both conditions simultaneously. However, identifying the presence of DFU solely based on its visual characteristics poses a significant challenge for clinicians. In many cases, DFU does not exhibit consistent shape and texture characteristics, making manual diagnosis unreliable [24], [25]. Manual diagnosis of DFU results in misdiagnosis in 2 out of every 3 cases. Therefore, it is imperative to harness advanced ML, DL, and computer vision techniques [26] to assist clinicians in accurately diagnosing DFU, thereby enhancing patient care. Developing an automatic diagnostic model can improve decision-making reliability at a minimal cost. While some research has been conducted in automatic DFU classification, there remains room for further investigation and development [27], [28].

Filipe et al. [16] introduced a two-stage ML classification approach that utilizes foot thermograms. At first, healthy and infected feet are distinguished [29]. In the next stage, assess the severity of the infection. However, the approach is costly and requires expertise to handle it. Goyal et al. [17] proposed DFUNet, a novel parallel convolution layer-based CNN architecture for differentiating between normal and abnormal DFU. DFUNet outperformed standard CNNs like LeNet, AlexNet, and GoogleNet, as well as traditional low-feature-based classification methods. However, the primary objective did not encompass identifying ischaemia in abnormal DFU wounds. Alzubaidi et al. [18] presented DFU_QUTNet, a CNN architecture for extracting multi-level features, which are subsequently input into Support Vector Machine (SVM) and K-Nearest Neighbours (KNN) classifiers. The method was compared to three standard CNN architectures (GoogleNet, AlexNet, and VGG16) to highlight its efficiency. Nonetheless, DFU_QUTNet did not address the identification of ischaemia in DFU cases. Another approach involved

TABLE I. Gap Analysis of DFU Diagnosis Approaches

Study	Focus	Methods	Gaps
Filipe et al. [16]	DFU severity classification	Two-stage ML with foot thermograms	High cost; Expertise required
Goyal et al. [17]	DFU classification	Parallel convolution layer-based CNN (DFUNet)	Does not address ischaemia
Alzubaidi et al. [18]	DFU feature extraction	CNN + SVM and KNN classifiers	Does not address ischaemia
Veredas et al. [19]	Necrotic tissue detection	NN + Bayesian Classifiers (BNC)	High false positive rate; Efficiency concerns
Scebba et al. [20]	Wound image segmentation	DL-based model	Requires minimization of false positives
Wang et al. [21]	Wound boundary determination	2-level SVM classifier	Inefficiencies in level 1 classifier
Ohura et al. [22]	DFU wound segmentation	Standard CNN architectures	Does not address ischaemia detection
Goyal et al. [23]	Ischaemia and infection recognition	Traditional ML-based techniques and CNN	Less promising infection vs. non-infection results
Chen et al. [30]	Healthcare with Federated Learning	FL integration in healthcare	Not specific to DFU
Fathima et al. [31]	FL in healthcare	FL integration with IoT	No FL integration in DFU monitoring

the hybridization of Neural Networks (NN) and Bayesian Classifiers (BNC) to detect necrotic tissue in wounds [19]. The NN model extracted color and texture features from segmented wound images, which BNC then processed for prediction. This method requires strategies to reduce false positive detections and enhance efficiency. Scebba et al. [20] proposed a DL-based model for wound image segmentation, with wound detection performed before segmentation to improve generalization. However, similar to the previous approach, this method necessitates strategies to minimize false positive detections and enhance efficiency. Wang et al. [21] introduced a 2-level SVM classifier for determining wound boundaries. Incorrectly identified samples from level 1 undergo further processing by the level 2 SVM classifier to enhance overall performance. In a study by Ohura et al. [22], standard CNN architectures were employed for DFU wound segmentation, with U-Net achieving the best results among LinkNet, U-Net_VGG16, SegNet, and U-Net. Nevertheless, this approach also requires addressing ischaemia identification. Goyal et al. [23] introduced a new dataset with ground truth labels for ischaemia and infection recognition. They applied various traditional ML-based feature extraction techniques [24] and CNN architectures to differentiate between ischaemia and infection as binary classification problems [25]. An ensemble approach demonstrated significant performance improvements in both tasks, although infection vs. non-infection results were less promising compared to ischaemia vs. non-ischaemia classification. However, FL's use in DFU research has not yet been explored. But, in the healthcare domain, FL gained attention [30], [31]. Haya et al. [32] proposed frameworks integrating FL and the Internet of Things (IoT) within the healthcare domain. They introduced a data integration approach for monitoring patients remotely through IoT without incorporating FL into the surveillance process. The work is assessed using ECG data, validating that DL surpassed other implemented algorithms in performance. The work efficiently integrated FL with an IoT digital system to uphold personal privacy. Sun et al. [33] advocated using FL to enhance the learning efficiency of IoT-based intelligent automation. Numerous researchers [34] proposed specialized federated learning paradigms for detecting COVID-19 cases using X-ray images. They applied transfer learning on pre-trained algorithms, with residual networks exhibiting superior performance. Rahman et al. [35] introduced an FL model for healthcare that incorporates a DL edge layer and blockchain to enhance security and reliability. A system for sharing industrial IoT data using FL and blockchain is also proposed. In addition [36], proposed FL method for Electronic Health Records (EHRs) in the healthcare domain, showcasing promising results. Baheti et al. [37], leveraging FL, employed CT scans to detect respiratory lung nodules. Huang et al. [38] utilized a clustering technique to generate community-based data with clinical relevance, with their clustering-based FL model surpassing the standard FL model in performance. They addressed the issue of non-IID (Non-Independently and Identically Distributed) ICU health information by grouping clients into significant clinical populations, thus enhancing fatality and ICU wait-time predictions. Furthermore, Lee et al. [39] developed a system for patient resemblance learning within a federated environment while safeguarding patient privacy. Their model can identify similar patients across healthcare centres, even when no records are shared. The related works are summarised in table I.

III. Problem Definition and System Model

A. Problem Definition

The DFU are among the most serious diabetic complications and consequences often resulting in. These include limb shortening through amputation or surgery, lasting nerve pain, or severe infections. This makes early identification and diagnosis more imperative, but modern diagnostic systems have several limitations.

1. Data Privacy Concerns: A central requirement for deploying traditional diagnostic models is data storage and management at one central location, creating room for security risks concerning privately held information, especially with sensitive medical information.

2. Infrastructure Limitations: Many medical institutions may not have the necessary equipment to consolidate and analyse large amounts of data.

3. Limited access to expensive diagnostic tools: The current diagnostic systems are often associated with the need for specialized imaging modalities and do not offer many possibilities that could be available in every primary care and low-resource setting.

The objective of this work consists of designing an intelligent and decentralized DFU diagnosis supporting system overcoming the above-mentioned challenges due to the improvement of privacy, decreased need for centralized data, and broadening diagnostic tools' availability.

B. System Model

To deal with the abovementioned challenges, this work presents a novel system model for diagnosing DFU based on federated learning. The system allows each client's devices, such as mobile phones, tablets and wearables, to build local machine-learning models using local data without sharing raw data with the central facility. The key elements of the system model are defined as follows:

1. Client-Side Architecture:
   - Each client contains a local DFU image dataset of diabetic patients.
   - The ResKNet architecture is employed on the client side for model training. ResKNet is designed to be lightweight, efficient, and perform well in resource-constrained environments.
   - Clients use a hybridized data augmentation approach to handle the class imbalance in their datasets, generating additional synthetic data for underrepresented classes.

2. Federated Learning Framework:
   - The central server orchestrates the training process by collecting only the model updates (weights and gradients) from each client, instead of raw data.
   - The server aggregates these updates using techniques such as Federated Averaging (FedAvg) and applies them to the global model.
   - This decentralized approach ensures that patient data remains local, significantly enhancing privacy and reducing the risk of data breaches.

3. Data Transmission:
   - Client devices periodically transmit their locally trained model updates to the central server. These updates are secured using encryption protocols to ensure the confidentiality of sensitive medical data further.
   - The system is robust to intermittent client connections, common in resource-constrained environments.

4. Global Model Update:
   - Once the central server aggregates the model updates from multiple clients, the global model is updated and sent back to the clients for further training and improvement.
   - This iterative process continues until the global model achieves satisfactory accuracy for DFU diagnosis across all clients.

5. Consumer Electronics Integration:
   - The system is designed to be integrated with consumer electronics such as smartphones, wearable devices, and tablets, making it accessible to a wide range of users in various healthcare settings, including remote or under-resourced areas.
   - The reliance on readily available consumer electronics mitigates the need for expensive diagnostic tools, enabling scalable deployment.

IV. Proposed Method

The proposed method employs DFU images for infection detection and ischaemia identification. The motivation for the proposed scheme arises from the need to tackle several critical challenges in diagnosing DFU and healthcare diagnostics in general. These challenges revolve around privacy concerns, class imbalances in medical datasets, resource constraints in healthcare settings, and the high costs associated with traditional diagnostic tools. The proposed scheme is designed with these specific challenges in mind, leveraging advanced machine learning techniques in a way that is both efficient and scalable. The primary goal is to show how FL enables the secure and privacy-preserving sharing of crucial private information in CE devices when integrated alongside a CNN architecture. The proposed FL architectural system in CE, depicted in Fig. 2, is connected to remote hospitals through intermittent clients. Fig. 2 visualizes the overall flow and structure of the federated learning system. The left side of the figure illustrates the local training process on the client devices. Each device performs model training using locally collected data and applies data augmentation to handle class imbalances. The middle section of the figure shows the process of sharing model updates with the central server. Instead of raw data, only the updated model parameters are transmitted, ensuring privacy protection. The right side of the figure demonstrates the aggregation process performed by the central server. The server collects the updates from all participating clients, applies the FedAvg technique, and updates the global model. This global model is then redistributed back to the clients and used as the basis for further local training. This entire process iterates, gradually improving the global model's ability to diagnose DFU accurately while maintaining data privacy and minimizing the need for expensive infrastructure or specialized medical devices. These remote hospitals provide DFU images for the training procedure. Data augmentation guarantees data balance before application in local training machines to create LMU. Every hospital supplies LMU to the centralized server through local training weights. The centralized server, akin to a hub in a CE system, collects LMU from many remote hospitals and combines them to generate GMU. The GMU is then returned to the hospitals for updating to achieve precise classification findings. This collaborative exchange is reminiscent of the resonance in CE ecosystems, where information is shared for shared development. This work extensively tested the suggested method, considering scenarios involving intermittent clients and diverse image samples to determine its usefulness and make the best classification performance feasible. The proposed technique for decentralized model training in DFU images utilizing the FL approach is divided into five steps. These processes involve collecting datasets, augmentation, dealing with intermittent clients, client-side model training, and server-side model aggregation.

A. Dataset Preparation

The dataset is accessed from Manchester Metropolitan University, London. The creators compile the dataset from Lancashire Teaching Hospitals, London. The dataset is divided into two subdirectories: DFU images for detecting ischaemia (dataset 1) and infection (dataset 2) images. Both tasks rely on binary classification, which can aid in evaluating DFU wounds by identifying Ischaemia and Infection. The dataset 1 initially had 1459 complete foot pictures (210 Ischaemia and 1249 Non-ischaemia). Then, 1666 patches are extracted with the region of interest (ROIs) in mind. In dataset 2, the initial number of whole foot photos was 1459 (628 infected and 831 non-infected), and 1666 patches were created from them. A few example image patches from both datasets are shown in Fig. 3.

B. Data Augmentation

The data augmentation approach can efficiently address overfitting concerns and enhance the model's overall outcomes. Recent research has seen the emergence of various innovative approaches to advance the data augmentation field. Each customer might possess diverse image samples within each category in this situation. Consequently, this could lead to the potential problem of class imbalance. The dataset is comprised of 628 samples of infectious nature and 831 samples classified as normal. The normal class contains more samples, whereas the infectious class has a minor representation. The class imbalance problem is solved with hybridized oversampling techniques combining strategies of SMOTE and SVM-SMOTE. At first, the samples are divided equally. Secondly, in the first half of the samples, SMOTE oversampling was used to generate minority samples diagonally by choosing a random minority sample and its K-nearest neighbours. Thirdly, the SVM-SMOTE oversampling method was applied to half of the samples left out. At last, separately generated synthetic samples are combined to get a balanced and more representative and balanced dataset. The data generation has been conducted in the following steps:
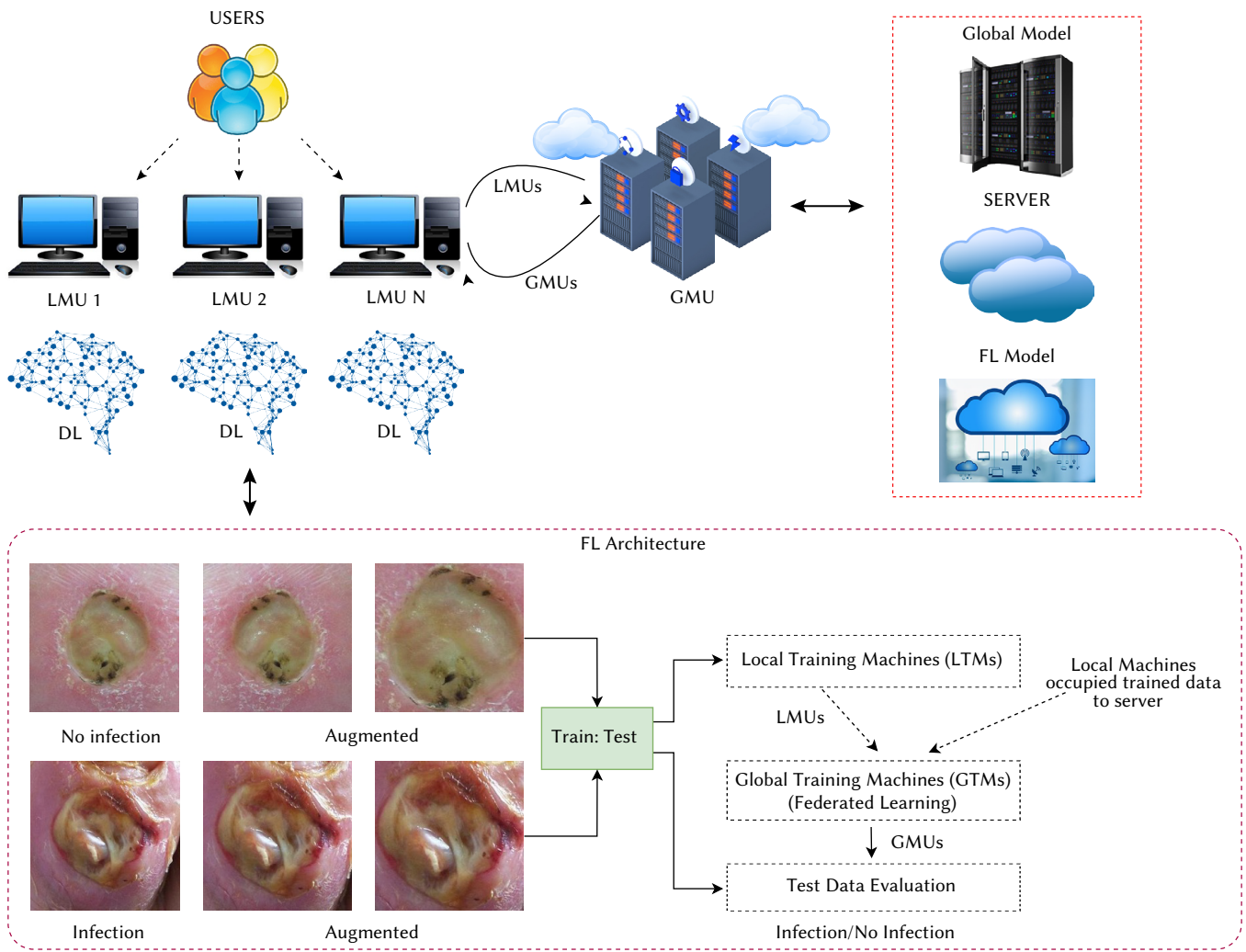
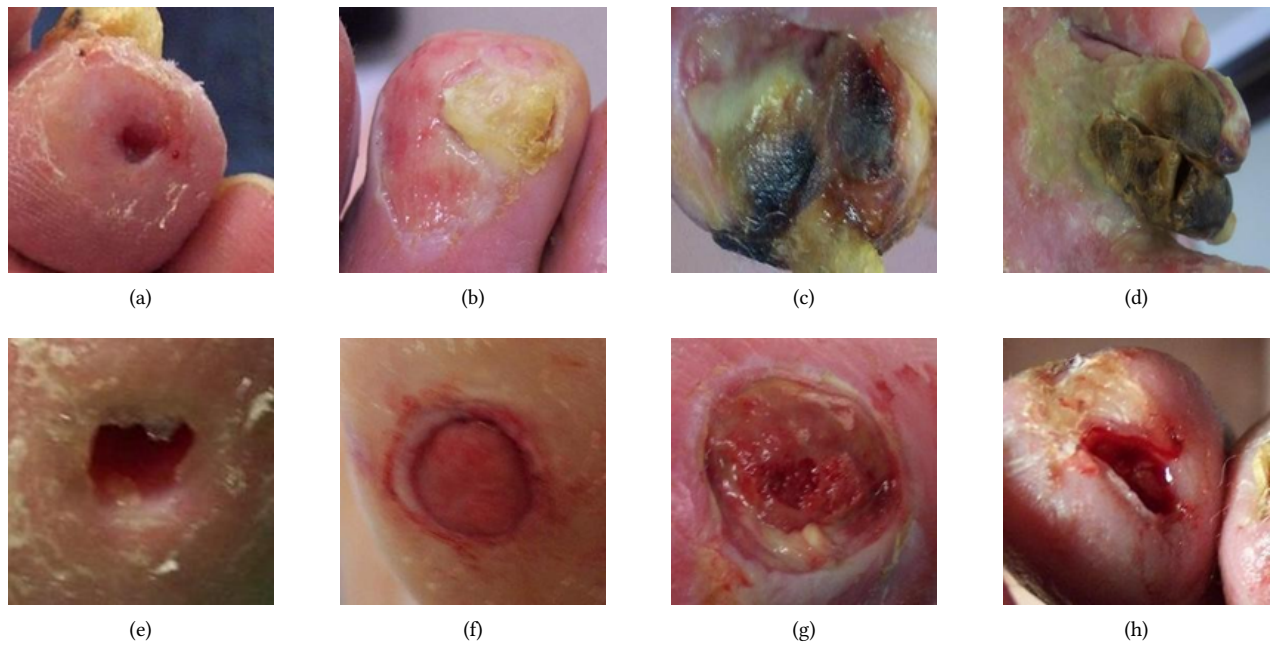Fig. 2. Overview of the federated learning framework for DFU diagnosis

Fig. 3. Example images: (a)-(b) Non-Ischaemia, and (c)-(d) Ischaemia images from DFU Ischaemia (dataset 1). (e)-(f) Non-Infection, and (g)-(h) Infection images from DFU Infection (dataset 2).

1. Divide the training samples T into T_1 and T_2, where $|T_1| = |T_2|$.

2. For each sample in T_1, do the following:

   - Choose any minority sample *'r'* from the feature space.

   - Select any instance *'m'* from the k nearest neighbors of *'r'*.

   - Generate a synthetic sample S_{SMOTE} along the line segment between *'r'* and *'m'*, where $S_{SMOTE} = r + w \times (m - r)$, and w is a random number in the range [0, 1].

3. For each sample in T_2, do the following:

   - Train an SVM with T_2 to find the decision boundary.

   - Choose a minority sample *'r'*.

   - Select any instance *'m'* from the k nearest neighbours of *'r'* within the decision boundary line segment.

   - If the number of majority samples among the k nearest neighbors is less than half:

     - Generate a synthetic sample $S_{SVMSMOTE}$ either above or below the line segment connecting *'m'* and *'r'* (extrapolation).

   - Else, generate a synthetic sample 's' between the line segment connecting *'m'* and *'r'* (interpolation).

4. Combine the synthetic samples generated in steps 2 and 3 to create a new set of training samples T'.

C. Irregular Clients

Several variables can contribute to the issue of infrequent clients. The most prevalent issues typically revolve around constraints in data transmission, network connections, and computing infrastructure [25]. Here, approaches are employed to address irregular clients, and the imbalance dataset is used.

- The proposed method is being tested on various clients, with some departing and others joining. The weights obtained during training sessions are not considered if a client departs from the system. The weights from the new client are integrated into the aggregation. In this scenario, the model performance is influenced by the image samples provided by the new client. This approach can yield improved classification results if the new client possesses sufficient picture samples for local training. However, it is important to note that new clients with fewer picture samples may negatively impact the aggregation weights.

- Upon a client's departure, its latest weights are retained and used in subsequent aggregations to update the model. The weights obtained from the most recent client are added to the aggregation, and the departing client's image samples are used to evaluate the model's performance.

D. CNN for Client-Side Model Training

On the client side, each FL client utilized personal data and local resources to execute mini-batch ADAM and local CNN training. The algorithm 1 is used for local client training. In algorithm 1, the inputs $Weight$ refer to the local model weight, and $Weight_T$ refers to the global model weight at round t. D_b is the data size in batches and DP_k is data points on client K. The local data trains the local model with collected weight $Weight_T$. Once the weights are collected, the updated $Weight_T$ the $Weight$ is updated. After iteratively running ADAM with local epochs aligned to create the most recent model update, the client computes a gradient update. The newly updated parameters are subsequently transmitted to the global server to update the data stored on the server. Further, the significant role played by the proposed CNN. The proposed CNN architecture, Res4Net, is designed as a shallow network with a deeper structure based on residual blocks. This network comprises a sequence of distinctive residual blocks involving 2D convolution, batch normalization, and LeakyReLU activation, connected by skip

connections (convolutional and identity). A visual representation of the model's layer-by-layer architecture can be observed in Fig. 4. The first residual block output block with skip connection can be defined mathematically from eq. (1).

$$Res4Net_{block(1/3)} = ADD[((Convskip_1^{W \times H \times D}, BN),$$
$$(Conv2D_1^{W \times H \times D}, BN, LR), (Conv2D_3^{W \times H \times D}, BN, LR),$$
$$(Conv2D_1^{W \times H \times D}, BN))]LR \tag{1}$$

The next consecutive residual block contains no skip connection and can be derived mathematically by eq. (2).

$$Res4Net_{block(2/4)} = ADD[((Conv2D_1^{W \times H \times D}, BN, LR),$$
$$(Conv2D_3^{W \times H \times D}, BN, LR), (Conv2D_1^{W \times H \times D}, BN))]LR \tag{2}$$

where $Res4Net_{block(1/3)}$ is the output of residual blocks 1 and 3. ADD represents addition operation $Convskip\_1^{W \times H \times D}$ is skip convolution layer with width W, height H, and D channel depth. The BN stands for batch normalization, and LR stands for leakyReLU activation function. After the convolution operation, The batch normalisation output will help balance input feature map distribution. The output of BN operation $Out_{B,C,X,Y}$ is derived in eq. (3).

$$Out_{B,C,X,Y} = \gamma_C \frac{Input_{B,C,X,Y} - \mu_C}{\sqrt{\sigma_C^2 + \epsilon}} + \beta_C \; \forall B, C, X, Y \tag{3}$$

where $Input_{B,C,X,Y}$ is a four-dimensional input with batch (B), Channel (C), X, and Y are spatial dimensions. The μ_C represents mean activation and β_C and σ_C are channel-wise affine transmission.

Algorithm 1: Client-Side Model Training (LMU)

Input: (**Weight**, **Weight**$_T$).

Output: Local Model Update (LMU) Weight

1: **Begin (Weight = Weight**$_T$)   // **Initialization**

2: **Spit** $D_b \leftarrow DP_K$, where D_b is batch data size and DP_K is data points for client K.

3: **Update Weight**$^{(T, D)}$ with ADAM optimizer and initial learning rate $1e - 2$.

4: **for** local epochs i from 1 to N: **do**   // **Beginning of outer for loop**

5:    **while** use optimizer: **do**   // **Optimizer loop**

6:      **for** every $D_{(bi)}$ in D_i: **do**   // **Data batch loop**

7:        **Find** $Global^D_{(bi)} \leftarrow \sigma D(\textbf{Weight}_b, N)$.   // **Global update**

8:        **Save Weight** $\leftarrow$ **Weight**$_b \leftarrow Global^D_{(bi)}$. / **Weight update**

9:      **end for**   // **End of data batch loop**

10:   **end while**   // **End of optimizer loop**

11: **end for**   // **End of outer for loop**

12: **return Weight** as LMU.   // **Return LMU**

E. FL Server-Side Model Aggregation

The LMU is the weight after training clients with irregular clients. The LMU from the client side forms GMU on the FL server side. The details of GMU formation are discussed in algorithm 2. If C_N is the client's number and C_k is the number of client data for k, $k \forall [1, ..., C_N]$, then the average weight from clients is calculated with eq. (4).

$$W_{avg(k)} = \frac{C_1}{\sum_{k=1}^{C_N} C_k} \tag{4}$$

The aggregated weights on the FL server side can be calculated using eq. (5).
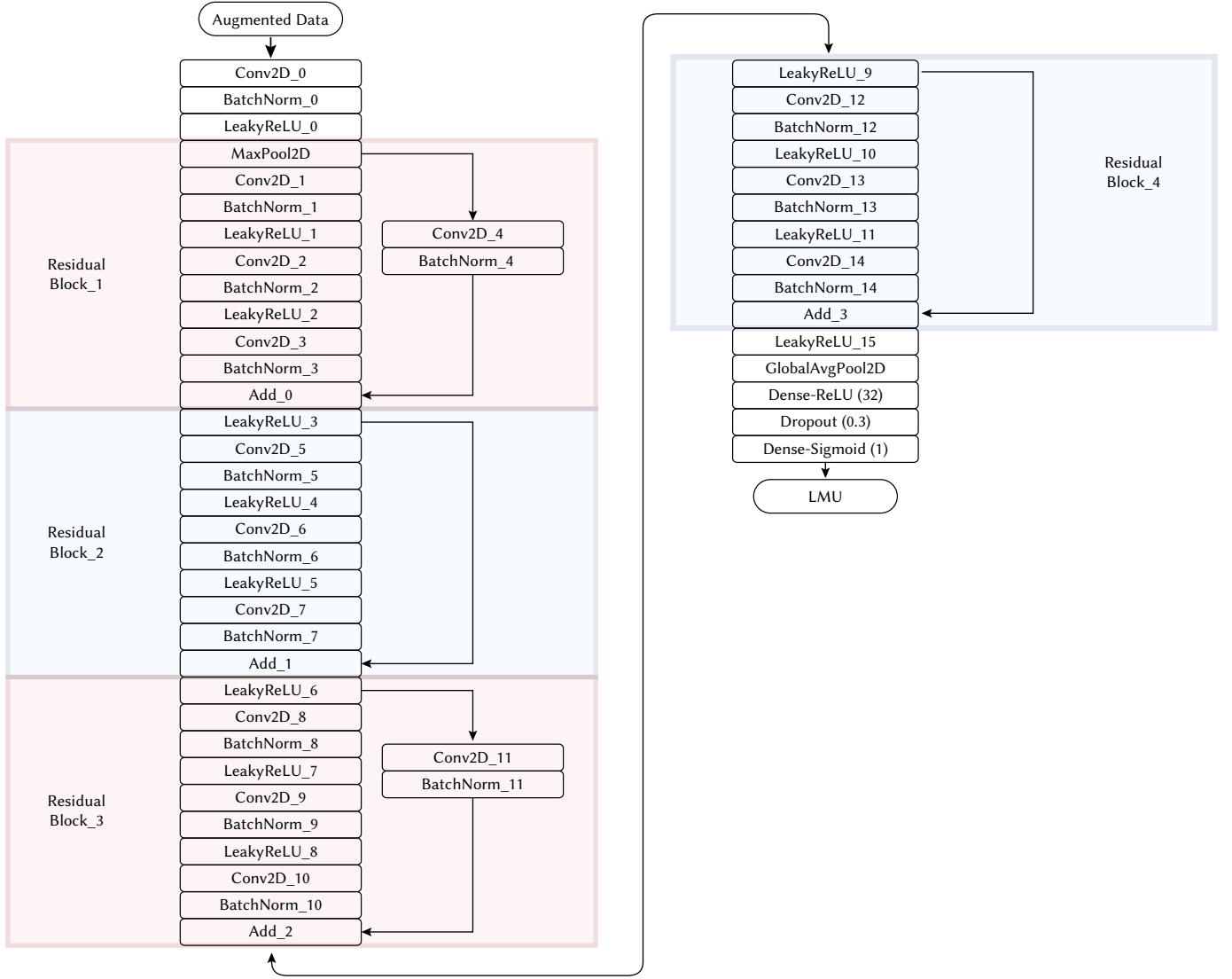
$$W_{aggregated} = \sum_{k=1}^{C_N} C_k W_k \tag{5}$$

Fig. 4. The proposed CNN (ResKNet) architecture for client training.

Algorithm 2: FL Server-Side Aggregation (GMU)

Input: **Weight**, FL_n (Federated cycles).

Output: **Weight**$_{agg}$, weight aggregation.

1: **Begin** $FL_n \leftarrow 0$, **Weight**^{0}, both cycles and weight initialized to 0.

2: **Compute** $M \leftarrow MAX(C \times k, 1)$ maximum clients.

3: **Select** I_t randomly of n clients at t cycle.

4: **while** $k \leftarrow I_t$: **do**   // **Beginning of while loop**

5:     Update weight **Weight**$_{t-1}$ to I_{t-1}.

6:     **Weight**$^t_{tk} \leftarrow update(t^k, $**Weight**$_{t-1})$.   // **Update current weight**

7: **end while**   // **End of while loop**

8: **Aggregation Weight**$_{agg} \leftarrow \sum_{t=1}^{t^k} \frac{n_t}{n}$**Weight**$^t_{tk}$.   // **Aggregating weights**

9: **return Weight**$_{agg}$

V. Performance Analysis

The proposed model performance is evaluated with the help of multiple important evaluation metrics. Further, the results are represented and analyzed with the help of various tables and graphs.

The following subsections include a detailed discussion of results evaluation and discussion.

A. Evaluation Metrics

The proposed approach is evaluated for varying-sized test data from intermittent clients. The proposed approach tested the capability of identification of infection vs. non-infection DFU wounds. Five evaluation metrics are recorded to check the performance of the proposed approach. The evaluation matrices considered Accuracy, Precision, Sensitivity, Specificity, and F1-Score are given in eqs. (6) - (10).

$$Accuracy = \frac{TP + TN}{TP + TN + FP + FN} \tag{6}$$

$$Precision = \frac{TP}{TP + FP} \tag{7}$$

$$Sensitivity/Recall = \frac{TP}{TP + FN} \tag{8}$$

$$Specificity = \frac{TN}{TN + FP} \tag{9}$$

$$F1 - Score = \frac{2 \times Precision \times Recall}{Precision + Recall} \tag{10}$$
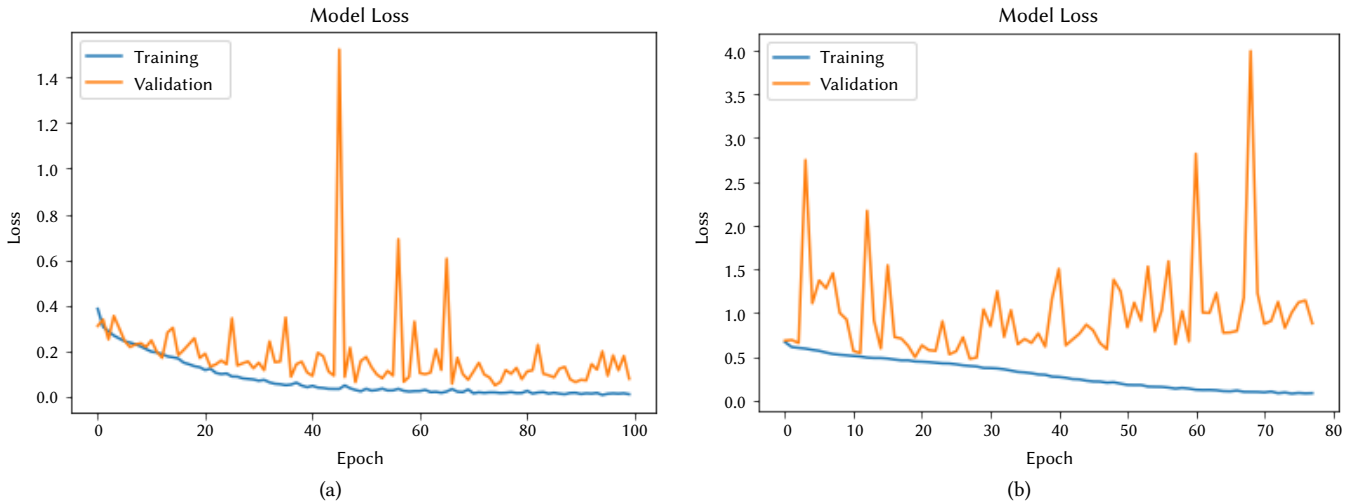
Fig. 5. Training and validation loss curve: (a) DFU Ischaemia (dataset 1). (b) DFU Infection (dataset 2).

TABLE II. Results With Different Clients Using Dataset 1

Class	Client	Precision	Sensitivity	Specificity	Accuracy	F1-Score
Ischaemia	5	96.44	97.43	96.46	96.90	97.47
Non-Ischaemia		96.74	96.84	96.97		
Ischaemia	10	97.15	97.20	97.18	97.25	97.55
Non-Ischaemia		97.06	97	97.07		
Ischaemia	15	98.37	98.67	98.38	98.73	98.41
Non-Ischaemia		97.87	98.27	97.88		
Ischaemia	20	99.18	99.49	99.20	99.50	99.36
Non-Ischaemia		98.98	99.18	99.00		

In eqs. (6)-(10), *TP* refers to True Positive, *TN* refers to True Negative, *FP* refers to False Positive, and *FN* refers to False Negative counts.

B. Results and Discussion

The data collected from consumer electronic devices to train an FL framework to learn from data can be analysed using various parameters. One such measure is the training vs. validation loss curve. The training vs. validation loss curves on the server side are shown in Fig. 5 for both datasets. Fig. 5 (a) is the loss curve for dataset 1 (ischaemia vs non-ischaemia), which shows training loss in blue coloured and validation loss in orange coloured. The training loss constantly decreases, but the validation loss shows a more dynamic nature. On the other hand, in the case of dataset 2, a more suitable training and validation loss curve is achieved. In Fig. 5 (b), for dataset 2, the training loss linearly decreases. However, in the case of validation loss, a sharp increase is observed in the 45th epoch. Additionally, the proposed method examines intermittent clients, selecting a certain amount of clients in every run while utilizing 300 instances from both datasets as the test data. Table II reports the classification results of dataset 1 for 5, 10,15, and 20 clients. In case 5 clients' classification between ischaemia and non-ischaemia, the precision, sensitivity, and specificity scores are 96.44%, 97.43%, and 96.46%, respectively. However, for non-ischaemia classes, a small improvement of the results is observed between 1-2% for 5 clients. Furthermore, the accuracy and F1-score values are the same for both classes at 96.90% and 97.47%, respectively. Similarly, for clients, 10 table II indicates that on increasing the number of clients to 10, classification performance increases. The classification results are improved (1-2)% compared to 5 clients. The results suggest that the sensitivity score of the non-ischaemia class is slightly higher than the ischaemia class. This is the reason for the larger value of false

negative counts. However, the interesting observation from table II is that an increase in client numbers increases the performance of the proposed system. The reason behind the performance improvement is an increase in client numbers reduces the load. Further, with 15 clients for dataset 1, the highest score in the ischaemia class is 98.37%, 98.67%, and 98.38% for precision, Sensitivity, and Specificity, respectively. These results are again better than 5 and 10 clients. Another important observation is that the proposed approach achieved higher performance in ischaemia identification than non-ischaemia identification for 15 clients. The last setup results with client 20 are reported in table II. The proposed approach achieved almost perfect results in identifying both ischaemia and non-ischaemia. In the case of the ischaemia class, the highest precision, recall, and specificity are 99.18%, 99.49%, and 99.20%, respectively. Similarly, with a small low score for the non-ischaemia class, the highest precision, sensitivity, and specificity scores are 98.99%, 99.18%, and 99.00%, respectively. The overall accuracy score is 99.50%, with an F1-Score of 98.41. Therefore, starting from 5 clients to 20 clients, the results are improved, which signifies that an increase in clients helps in better learning and thereby improves performance.

Result table III shows the performance of the proposed approach with 5, 10, 15, and 20 clients in dataset 2. The classification results of infection are poor compared to the ischaemia classification. The highest results for the infection class in terms of precision, recall, and specificity are 85.90%, 82.81%, and 85.36%, respectively. Similarly, table III shows results with 10 clients for dataset 2. In the case of dataset 2 for infection and non-infection, both classes show a sharp increase in results. The results are improved by more than 3%. However, in the case of 10 clients, the identification results of the non-infection class slightly decreased.

TABLE III. RESULTS WITH DIFFERENT CLIENTS USING DATASET 2

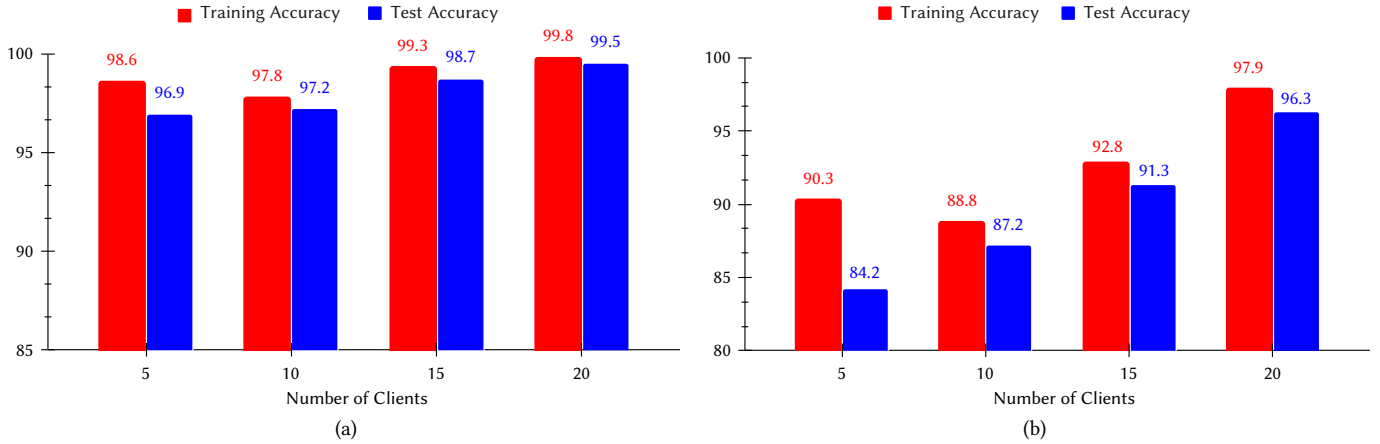| Class	Client	Precision	Sensitivity	Specificity	Accuracy	F1-Score
Infection	5	85.90	82.81	85.36	84.04	84.86
Non-Infection		86.80	83.46	86.42		
Infection	10	88.59	83.73	88.18	87.09	85.33
Non-Infection		88.03	84.28	87.65		
Infection	15	92.84	89.19	92.59	91.34	90.32
Non-Infection		91.92	87.56	91.71		
Infection	20	99.95	94.10	97.02	96.26	94.49
Non-Infection		95.55	91.65	96.47		

Fig. 6. The training and test accuracy on different numbers of clients: (a) DFU Ischaemia (dataset 1). (b) DFU Infection (dataset 2).

Once the number of clients further increased to 15, the performance of the proposed approach improved, as shown in table III. But the increment is quite promising, with an average value of (4-5)%. In the case of infection identification, the results are reported as 92.84%, 89.19%, and 92.59% for precision, sensitivity and specificity. The improvement in sensitivity score is lower than the other two evaluation metrics due to the large count of false negative values. Similarly, an improvement is observed in the case of non-infection identification compared to 10 clients. However, the improvement is slightly lower than the infection class. The identification of positive class always has a higher priority in medical diagnosis.

The last records in table III show the results of dataset 2 with 20 clients. There is a significant improvement in both infection and non-infection identification. The results with 20 clients are (4-7)% higher than 15 clients. Also, the results are improved to around 4% for the non-infection class. The increase in clients helps improve the results of the proposed approach. However, in the case of dataset 2, where identification of the correct class is more complex than dataset 1, there are more improvements. Further, the training and test accuracy in the line graph for different client numbers (dataset 1) is shown in Fig. 6 (a). The difference between training accuracy and test accuracy reduces the client number is increased. Similarly, Fig. 6 (b) shows the train and test accuracy for different clients in dataset 2. The characteristic of the line graph is similar to dataset 1. The reduction in train and test accuracy differences from 10 clients shows that the model learns very well and provides more generalization once the client numbers are increased.

In FL architecture, collaborating hospitals can produce LMUs using a variety of image sets as test data. Therefore, evaluating the proposed approach with random test data is very important. The proposed model is analyzed using varied test data sizes from both datasets. The results for dataset 1 on taking various image sample sizes are reported in table IV. The different numbers of image test samples are taken as 200, 150, 100, and 50. In the case of 200 test samples, the overall accuracy is 98.22%, and the F1-score is 98.91%. The precision, sensitivity and specificity scores in the ischaemia class are slightly higher than the non-ischaemia class. Further, when the test sample size is reduced to 150, the overall accuracy and F1-score scores are reduced to 97.46% and 97.05%, respectively. Similar characteristics are observed in the case of ischaemia and non-ischaemia, where precision, sensitivity and precision are reduced by around 1%. The highest overall accuracy and F1 scores are achieved for a test sample size of 100 with the values of 99.54% and 99.12%, respectively. With 100 test sample size, the performance of ischemia identification is better than non-ischaemia identification. In the case of ischaemia identification, the highest sensitivity score is 99.08%. Similarly, the scores of precision and specificity are 99.18% and 99.10%, respectively. The performance of non-ischaemia with a 100 test sample size is slightly reduced, but it is the highest result among other test sample sizes. The precision and sensitivity scores for non-ischaemia are 98.77%. The specificity score is also almost the same, with a value of 98.80%. Further, when the test sample is reduced to 50, the overall accuracy and F1-score outperformed compared to the 200 and 150 sample sizes. More specifically, with an accuracy of 99.03%, it is the second-best performing sample size. The sensitivity score of the ischaemia class is 98.67%, whereas for non-ischaemia, it is 98.27%. The results of considered test samples for dataset 2 are reported in table V. Similar characteristics are observed for infection vs. non-infection datasets as well. The overall accuracy and F1-score of 200 and 150 test samples are poor compared to 100 and 50 sample sizes. In the case of 200 test samples, the accuracy score is achieved as 85.86%, Which is further reduced to 83.71% with a 150 sample size. The F1-score for 200 samples is reported as 85.52%, and the lowest F1-score of 81.05% is reported with a 150 sample size. In individual classes, the precision, recall, and specificity scores for infection are 86.58%, 83.46%, and 86.06%,

TABLE IV. Results With Different Test Data Size Using Dataset 1

Class	Client	Precision	Sensitivity	Specificity	Accuracy	F1-Score
Ischaemia	200	97.67	98.16	97.69	98.22	98.91
Non-Ischaemia		97.36	97.86	97.39		
Ischaemia	150	96.67	97.45	96.69	97.46	97.05
Non-Ischaemia		96.16	96.84	96.19		
Ischaemia	100	99.08	99.18	99.10	99.54	99.12
Non-Ischaemia		98.77	98.77	98.80		
Ischaemia	50	98.57	98.67	98.60	99.03	98.61
Non-Ischaemia		98.27	98.27	98.30		

TABLE V. Results With Different Test Data Size Using Dataset 2

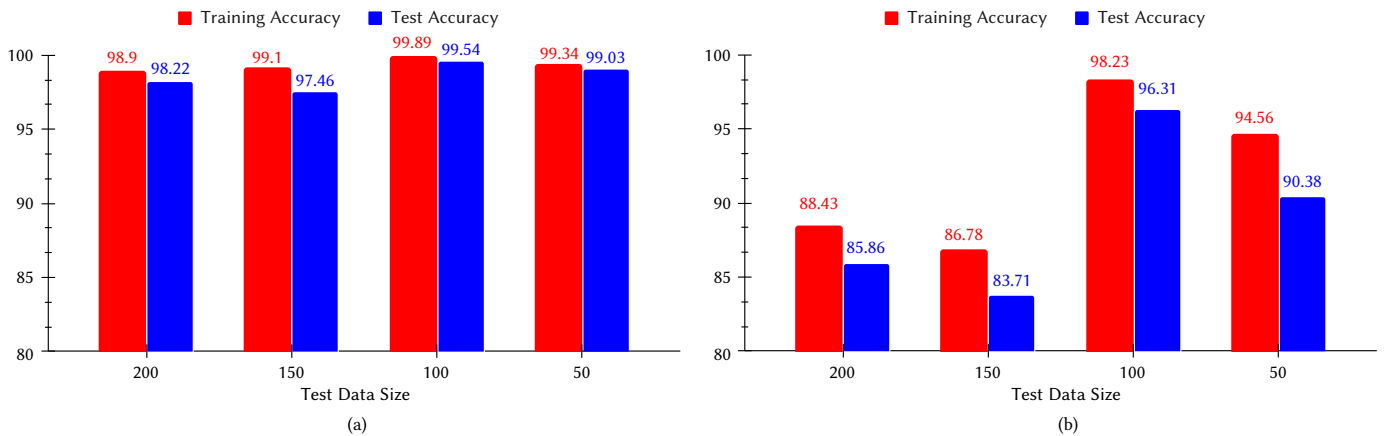| Class	Client	Precision	Sensitivity	Specificity	Accuracy	F1-Score
Infection	200	86.58	83.46	86.06	85.86	85.52
Non-Infection		87.24	83.96	86.06		
Infection	150	84.51	82.16	83.77	83.71	81.05
Non-Infection		85.13	82.48	83.06		
Infection	100	97.10	93.28	97.00	96.31	94.51
Non-Infection		96.25	92.47	96.11		
Infection	50	90.83	87.56	90.31	90.38	88.01
Non-Infection		89.98	86.74	89.59		

Fig. 7. The training and test accuracy on different test data sizes: (a) DFU Ischaemia (dataset 1). (b) DFU Infection (dataset 2).

respectively, with 200 samples. These scores slightly improved for the non-ischaemia class with around 1%. Among all considered sample size settings, the highest results are reported with a 100-test sample size. The overall accuracy and F1-score are 96.31% and 94.51%, respectively. In the case of infection with 100 samples, the highest precision, sensitivity and specificity results are 97.10%, 93.28%, and 97.00%. A slightly low sensitivity score compared to precision and specificity is due to a somewhat high value of false negative count. Similarly, in the case of non-infection identification, the results are impressive, with a slight decrement around (1-2)% compared to infection. The second-best result is achieved with a sample size of 50, where the accuracy and F1-Score are 90.38% and 88.01%. The evaluation of different test data sizes for dataset 1 and dataset 2 is shown in Figs. 7 (a) and 7 (b), respectively. The difference between training and test accuracy for 200 and 150 is higher than 100 and 50 in both datasets. Therefore, the observation from these tables is that the proposed approach can greatly help evaluate small sample sizes in real-life clinical practice. Fig. 8 shows the comparison of the proposed approach in terms of

accuracy and F1-Scores with state-of-the-art works. The proposed approach outperforms the popular standard CNNs. The significant improvements of the proposed work with nearly (4-9)% of accuracy in dataset 1 and (2-24)% in dataset 2 shows its importance in diagnosing the disease.

VI. Conclusions

This paper presents a federated learning-based approach for the automatic diagnosis of DFU, addressing key challenges such as data privacy and diagnostic accuracy. By leveraging a decentralized learning framework, this work enables training machine learning models directly on client devices, such as smartphones and tablets, without transferring sensitive patient data to a central server. This approach significantly mitigates privacy concerns commonly associated with centralized data processing in healthcare. Furthermore, the proposed approach introduces a hybridized data augmentation technique to handle class imbalance in DFU datasets, improving the model's ability
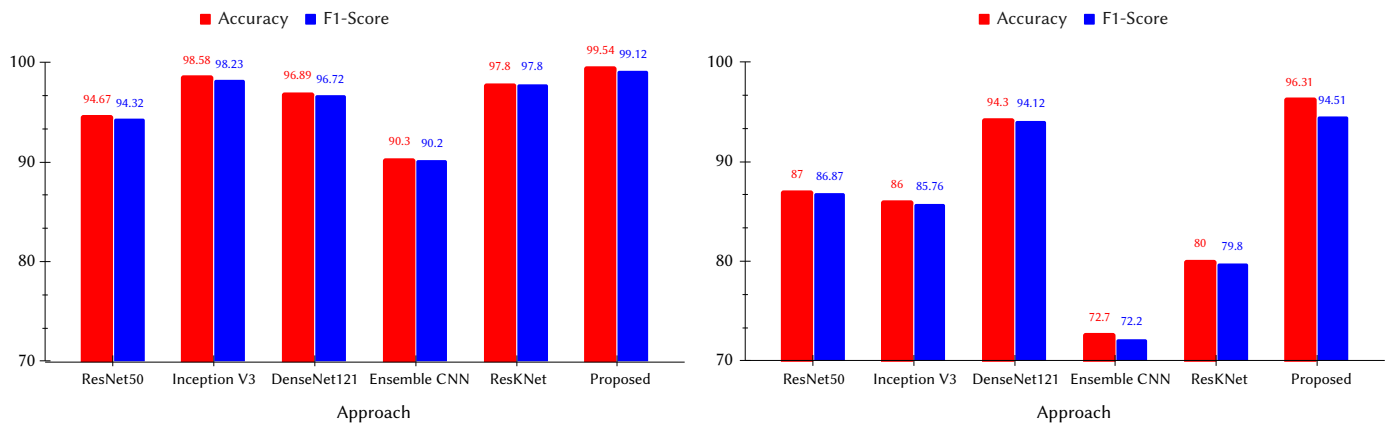
Fig. 8. Comparison with SOTA works: (a) DFU Ischaemia (dataset 1). (b) DFU Infection (dataset 2).

to classify ischaemia and infection in DFU. Using lightweight CNN (ResKNet) demonstrates the feasibility of running effective models even on resource-constrained devices, offering a practical solution for real-world healthcare applications. The result shows that the federated learning system achieved strong performance across multiple communication rounds, with continuous improvements in accuracy and reductions in model loss. The system's effectiveness is further validated with high precision in correctly classifying DFU stages, with minimal false positives and false negatives. This performance, coupled with the system's scalability and ability to function in low-resource environments, underlines its potential for widespread deployment in developed and developing regions. Ultimately, the proposed approach has the potential to provide accessible, affordable, and privacy-preserving diagnostic support for DFU patients. Future research could expand on this work by exploring more sophisticated data augmentation techniques to further enhance model performance, particularly in scenarios with more severe class imbalances. Applying the federated learning framework to other medical domains may improve data privacy and diagnostic accuracy across various conditions. These developments could help strengthen the impact of federated learning in healthcare, making it a key enabler for secure and effective medical diagnostics in diverse settings.

VII. Declaration of Competing Interest

The authors declare that they have no conflict of interest.

VIII. Authors Contribution Statement

Sujit Kumar Das is the main author of this paper, who has conceived the idea and discussed it with all co-authors. He has developed all the algorithms. Nageswara Rao Moparthi and Suyel Namasudra have performed the simulations of this paper. Rubén González Crespo is the corresponding author, who has supervised the entire work and proofread the paper. David Taniar has evaluated the performance and write-up of this work.

IX. Compliance With Ethical Standards

The authors did not use animals and human participants in the study reported in this work.

X. Data Availability

The data that support the findings of this study are available with the authors, but restrictions apply to the availability of these data.

Thus, data are not publicly available. However, data are available with permission from the Department of Computing and Mathematics, Manchester Metropolitan University, UK.

XI. Funding

The authors did not receive financial support from any organization for the submitted work.

References

[1] A. K. Mishra, P. Roy, S. Bandyopadhyay, S. K. Das, "Feature fusion based machine learning pipeline to improve breast cancer prediction," *Multimedia Tools and Applications*, vol. 81, no. 26, pp. 37627–37655, 2022, doi: 10.1007/s11042-022-13498-4.

[2] S. Saminu, G. Xu, S. Zhang, I. Ab El Kader, H. A. Aliyu, A. H. Jabire, Y. K. Ahmed, M. J. Adamu, "Applications of artificial intelligence in automatic detection of epileptic seizures using eeg signals: A review," in *Artificial Intelligence and Applications*, vol. 1, 2023, pp. 11–25.

[3] S. Jiang, Y. Gu, E. Kumar, "Magnetic resonance imaging (mri) brain tumor image classification based on five machine learning algorithms," *Cloud Computing and Data Science*, vol. 4, pp. 122–133, 2023, doi: 10.37256/ccds.4220232740.

[4] R. J. Robinson, "Insights on cloud security management," *Cloud Computing and Data Science*, vol. 4, pp. 212–222, 2023, doi: 10.37256/ccds.4220233292.

[5] J. Purohit, R. Dave, "Leveraging deep learning techniques to obtain efficacious segmentation results," *Archives of Advanced Engineering Science*, vol. 1, no. 1, pp. 11–26, 2023, doi: 10.47852/bonviewAAES32021220.

[6] P. Voigt, A. Von dem Bussche, "The eu general data protection regulation (gdpr)," *A Practical Guide, 1st Ed., Cham: Springer International Publishing*, vol. 10, no. 3152676, pp. 10–5555, 2017, doi: 10.1007/978-3-319-57959-7.

[7] S. Namasudra, P. Roy, "Size based access control model in cloud computing," in *Proc. of the International Conference on Electrical, Electronics, Signals, Communication and Optimization*, 2015, pp. 1–4.

[8] A.-R. Al-Ali, I. A. Zualkernan, M. Rashid, R. Gupta, M. AliKarar, "A smart home energy management system using iot and big data analytics approach," *IEEE Transactions on Consumer Electronics*, vol. 63, no. 4, pp. 426–434, 2017, doi: 10.1109/TCE.2017.015014.

[9] S. H. Requena, J. M. G. Nieto, A. Popov, I. N. Delgado, "Human activity recognition from sensorised patient's data in healthcare: A streaming deep learning-based approach," *IJIMAI*, vol. 8, no. 1, pp. 23–37, 2023, doi: https://hdl.handle.net/10630/27669.

[10] Y. He, X. Jin, Q. Jiang, Z. Cheng, P. Wang, W. Zhou, "Lkat-gan: A gan for thermal infrared image colorization based on large kernel and attentionunet-transformer," *IEEE Transactions on Consumer Electronics*, vol. 69, no. 3, pp. 478 – 489, 2023, doi: 10.1109/TCE.2023.3280165.

[11] F. Ullah, G. Srivastava, H. Xiao, S. Ullah, J. C.- Lin, Y. Zhao, "A scalable federated learning approach for collaborative smart healthcare systems with intermittent clients using medical imaging," *IEEE Journal of Biomedical and Health Informatics*, 2023, doi: 10.1109/JBHI.2023.3282955.

[12] Z. Zhang, Y. Li, Y. Gong, Y. Yang, S. Ma, X. Guo, S. Ercisli, "Dataset and baselines for iid and ood image classification considering data quality and evolving environments," vol. 8, 2023, doi: 10.9781/ijimai.2023.01.007.

[13] H. Guan, P.-T. Yap, A. Bozoki, M. Liu, "Federated learning for medical image analysis: A survey," *Pattern Recognition*, p. 110424, 2024, doi: 10.1016/j.patcog.2024.110424.

[14] V. Stephanie, I. Khalil, M. Atiquzzaman, X. Yi, "Trustworthy privacy-preserving hierarchical ensemble and federated learning in healthcare 4.0 with blockchain," *IEEE Transactions on Industrial Informatics*, vol. 19, pp. 7936 – 7945, 2022, doi: 10.1109/TII.2022.3214998.

[15] S. K. Das, S. Namasudra, A. K. Sangaiah, "Hcnnet: hybrid convolution neural network for automatic identification of ischaemia in diabetic foot ulcer wounds," *Multimedia Systems*, vol. 30, no. 1, p. 36, 2024, doi: 10.1007/s00530-023-01241-4.

[16] V. Filipe, P. Teixeira, A. Teixeira, "Automatic classification of foot thermograms using machine learning techniques," *Algorithms*, vol. 15, no. 7, p. 236, 2022, doi: 10.3390/a15070236.

[17] M. Goyal, N. D. Reeves, A. K. Davison, S. Rajbhandari, J. Spragg, M. H. Yap, "Dfunet: Convolutional neural networks for diabetic foot ulcer classification," *IEEE Transactions on Emerging Topics in Computational Intelligence*, vol. 4, no. 5, pp. 728–739, 2018, doi: 10.1109/TETCI.2018.2866254.

[18] L. Alzubaidi, M. A. Fadhel, S. R. Oleiwi, O. Al- Shamma, J. Zhang, "Dfu_qutnet: diabetic foot ulcer classification using novel deep convolutional neural network," *Multimedia Tools and Applications*, vol. 79, no. 21, pp. 15655–15677, 2020, doi: 10.1007/s11042-019- 07820-w.

[19] F. Veredas, H. Mesa, L. Morente, "Binary tissue classification on wound images with neural networks and bayesian classifiers," *IEEE transactions on medical imaging*, vol. 29, no. 2, pp. 410–427, 2009, doi: 10.1109/TMI.2009.2033595.

[20] G. Scebba, J. Zhang, S. Catanzaro, C. Mihai, O. Distler, M. Berli, W. Karlen, "Detect-and-segment: a deep learning approach to automate wound image segmentation," *Informatics in Medicine Unlocked*, vol. 29, p. 100884, 2022, doi: 10.1016/j.imu.2022.100884.

[21] L. Wang, P. C. Pedersen, E. Agu, D. M. Strong, B. Tulu, "Area determination of diabetic foot ulcer images using a cascaded two-stage svm-based classification," *IEEE Transactions on Biomedical Engineering*, vol. 64, no. 9, pp. 2098–2109, 2016, doi: 10.1109/TBME.2016.2632522.

[22] N. Ohura, R. Mitsuno, M. Sakisaka, Y. Terabe, Y. Morishige, A. Uchiyama, T. Okoshi, I. Shinji, A. Takushima, "Convolutional neural networks for wound detection: the role of artificial intelligence in wound care," *Journal of wound care*, vol. 28, no. Sup10, pp. S13–S24, 2019, doi: 10.12968/jowc.2019.28.Sup10.S13.

[23] M. Goyal, N. D. Reeves, S. Rajbhandari, N. Ahmad, C. Wang, M. H. Yap, "Recognition of ischaemia and infection in diabetic foot ulcers: Dataset and techniques," *Computers in Biology and Medicine*, vol. 117, p. 103616, 2020, doi: 10.1016/j.compbiomed.2020.103616.

[24] V. Rajinikanth, S. Kadry, P. Moreno-Ger, "Resnet18 supported inspection of tuberculosis in chest radiographs with integrated deep, lbp, and dwt features," *International Journal of Interactive Multimedia and Artificial Intelligence (IJIMAI)*, vol. 8, pp. 38–46, 2023, doi: 10.9781/ijimai.2023.05.004.

[25] A. Gupta, S. Namasudra, "A novel technique for accelerating live migration in cloud computing," *Automated Software Engineering*, vol. 29, no. 1, p. 34, 2022, doi: 10.1007/s10515-022-00332-2.

[26] V. Singh, D. Jain, "A hybrid parallel classification model for the diagnosis of chronic kidney disease," vol. 8, 2023, doi: 10.9781/ijimai.2021.10.008.

[27] J.-H. Ahn, Y. Ma, S. Park, C. You, "Federated active learning (f-al): an efficient annotation strategy for federated learning," *IEEE Access*, 2024, doi: 10.1109/ACCESS.2024.3376746.

[28] D. Li, W. Xie, Z. Wang, Y. Lu, Y. Li, L. Fang, "Feddiff: Diffusion model driven federated learning for multi-modal and multi-clients," *IEEE Transactions on Circuits and Systems for Video Technology*, 2024, doi: 10.1109/TCSVT.2024.3407131.

[29] S. A. Rieyan, M. R. K. News, A. M. Rahman, S. A. Khan, S. T. J. Zaarif, M. G. R. Alam, M. M. Hassan, M. Ianni, G. Fortino, "An advanced data fabric architecture leveraging homomorphic encryption and federated learning," *Information Fusion*, vol. 102, p. 102004, 2024, doi: 10.1016/j.inffus.2023.102004.

[30] S. Chen, L. Li, G. Wang, M. Pang, C. Shen, "Federated learning with heterogeneous quantization bit allocation and aggregation for internet of things," *IEEE Internet of Things Journal*, vol. 11, pp. 3132–3143, 2023, doi: 10.1109/JIOT.2023.3296493.

[31] M. D. Fathima, S. J. Samuel, S. Raja, "Hddss: An enhanced heart disease decision support system using rfe-abgnb algorithm.," *International Journal of Interactive Multimedia & Artificial Intelligence*, no. 527, 2023, doi: 10.9781/ijimai.2021.10.003.

[32] H. Elayan, M. Aloqaily, M. Guizani, "Sustainability of healthcare data analysis iot-based systems using deep federated learning," *IEEE Internet of Things Journal*, vol. 9, no. 10, pp. 7338–7346, 2021, doi: 10.1109/JIOT.2021.3103635.

[33] W. Sun, S. Lei, L. Wang, Z. Liu, Y. Zhang, "Adaptive federated learning and digital twin for industrial internet of things," *IEEE Transactions on Industrial Informatics*, vol. 17, no. 8, pp. 5605–5614, 2020, doi: 10.1109/TII.2020.3034674.

[34] Z. Li, X. Xu, X. Cao, W. Liu, Y. Zhang, D. Chen, H. Dai, "Integrated cnn and federated learning for covid-19 detection on chest x-ray images," *IEEE/ACM Transactions on Computational Biology and Bioinformatics*, vol. 21, pp. 835 – 845, 2022, doi: 10.1109/TCBB.2022.3184319.

[35] M. A. Rahman, M. S. Hossain, M. S. Islam, N. A. Alrajeh, G. Muhammad, "Secure and provenance enhanced internet of health things framework: A blockchain managed federated learning approach," *Ieee Access*, vol. 8, pp. 205071–205087, 2020, doi: 10.1109/ACCESS.2020.3037474.

[36] T. K. Dang, X. Lan, J. Weng, M. Feng, "Federated learning for electronic health records," *ACM Transactions on Intelligent Systems and Technology (TIST)*, vol. 13, no. 5, pp. 1–17, 2022, doi: 10.1145/3514500.

[37] P. Baheti, M. Sikka, K. Arya, R. Rajesh, "Federated learning on distributed medical records for detection of lung nodules.," in *VISIGRAPP (4: VISAPP)*, 2020, pp. 445–451.

[38] L. Huang, A. L. Shea, H. Qian, A. Masurkar, H. Deng, D. Liu, "Patient clustering improves efficiency of federated machine learning to predict mortality and hospital stay time using distributed electronic medical records," *Journal of biomedical informatics*, vol. 99, p. 103291, 2019, doi: 10.1016/j.jbi.2019.103291.

[39] J. Lee, J. Sun, F. Wang, S. Wang, C.-H. Jun, X. Jiang, *et al.*, "Privacy-preserving patient similarity learning in a federated environment: development and analysis," *JMIR medical informatics*, vol. 6, no. 2, p. e7744, 2018, doi: 10.2196/medinform.7744.

Sujit Kumar Das

Sujit Kumar Das received a Ph.D. from the Department of Computer Science and Engineering, National Institute of Technology Silchar, India. Currently, he works as an Assistant Professor in the Department of Computer Science and Engineering, Institute of Technical Education and Research, Siksha 'O' Anusandhan Deemed to be University, Bhubaneswar, Odisha, India. His research interests include deep learning, computer vision, and medical imaging. He has published 15 SCI/SCOPUS-indexed journal articles. Dr. Das is also an active reviewer in the domain o medical imaging, deep learning, and computer vision.

Nageswara Rao Moparthi

Nageswara Rao Moparthi is a Professor at the Amrita Vishwa Vidyapeetham, Andhra Pradesh, India, in the Amrita School of Computing. Machine learning with software engineering techniques was his doctorate's major domain/specialization. His research areas include data mining, data analytics, machine learning, soft engineering and IoT. Prof. Rao has around 13 years of IT industry exposure and 7 years of teaching cum research experience. He is an active reviewer of many reputed journals and published research papers in many SCI-indexed journals. He is also an organizing committee member/TPC member of many international conferences.

Suyel Namasudra

Suyel Namasudra has received Ph.D. degree from the National Institute of Technology Silchar, Assam, India. He was a post-doctorate fellow at the International University of La Rioja (UNIR), Spain. Currently, Dr. Namasudra is working as an assistant professor in the Department of Computer Science and Engineering at the National Institute of Technology Agartala, Tripura, India. Before joining the National Institute of Technology Agartala, Dr. Namasudra was an assistant professor in the Department of Computer Science and Engineering at the National Institute of Technology Patna, Bihar, India. His research interests include blockchain technology, cloud computing, DNA computing, and information security. Dr. Namasudra has edited 8 books, 5 patents, and 87 publications in conference proceedings, book chapters, and refereed journals like IEEE TII, IEEE TNSM, IEEE TCE, IEEE T-ITS, IEEE TSC, IEEE TCSS, IEEE TCBB, ACM TOMM, ACM TOSN, ACM TALLIP, FGCS, CAEE, and many more. He is the Editor-in-Chief of the Cloud Computing and Data Science (ISSN: 2737-4092 (online)) journal. Dr. Namasudra has served as a Lead Guest Editor/Guest Editor in many reputed journals like IEEE TCE (IEEE, IF: 4.3), IEEE TBD (IEEE, IF: 7.2), ACM TOMM (ACM, IF: 3.144), MONET (Springer, IF: 3.426), CAEE (Elsevier, IF: 3.818), CAIS (Springer, IF: 4.927), CMC (Tech Science Press, IF: 3.772), Sensors (MDPI, IF: 3.576), and many more. He has also participated in many international conferences as an organizer and session chair. Dr. Namasudra is a senior member of IEEE and ACM. He has been featured in the list of the top 2% scientists in the world from 2021 to 2024. His h-index is 39.

Rubén González Crespo

Ruben Gonzalez Crespo has received PhD in Computer Science Engineering. He is the Vice-Rector of Academic and Professorate Affairs of UNIR, Spain. He is the Editor-in-Chief of the International Journal of Interactive Multimedia and Artificial Intelligence and an editorial board member of many indexed journals. His main research areas are Soft Computing, Accessibility and TEL. He is an advisory board member of the Ministry of Education, Colombia and an evaluator of the National Agency for Quality Evaluation and Accreditation of Spain (ANECA)

David Taniar

David Taniar received all his degrees (Bachelor, Master, and PhD) in Computer Science. His research expertise includes data warehousing, data management, data engineering, and data analytics. His recent book on Data Warehousing and Analytics (Springer, 2021) has been accessed more than 50 thousand times and is being used as a textbook worldwide. He has graduated more than 25 PhD students in his career. He is currently an Associate Professor at Monash University, Australia.